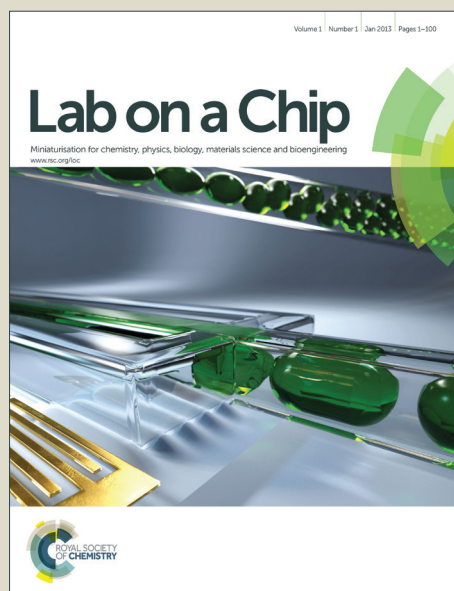


# Lab on a Chip

Accepted Manuscript



This article can be cited before page numbers have been issued, to do this please use: M. Ebrahimi Warkiani, A. K. P. Tay, B. L. Khoo, X. Xiaofeng, C. T. Lim and J. Han, *Lab Chip*, 2014, DOI:



This is an *Accepted Manuscript*, which has been through the Royal Society of Chemistry peer review process and has been accepted for publication.

*Accepted Manuscripts* are published online shortly after acceptance, before technical editing, formatting and proof reading. Using this free service, authors can make their results available to the community, in citable form, before we publish the edited article. We will replace this *Accepted Manuscript* with the edited and formatted *Advance Article* as soon as it is available.

You can find more information about *Accepted Manuscripts* in the [Information for Authors](#).

Please note that technical editing may introduce minor changes to the text and/or graphics, which may alter content. The journal's standard [Terms & Conditions](#) and the [Ethical guidelines](#) still apply. In no event shall the Royal Society of Chemistry be held responsible for any errors or omissions in this *Accepted Manuscript* or any consequences arising from the use of any information it contains.

# Malaria detection using inertial microfluidics

Majid Ebrahimi Warkiani<sup>1,2#</sup>, Andy Kah Ping Tay<sup>1#</sup>, Bee Luan Khoo<sup>3,4</sup>, Xu Xiaofeng<sup>4</sup>, Jongyoon Han<sup>1,5\*</sup>, Chwee Teck Lim<sup>1,3,4\*</sup>

<sup>1</sup>BioSystems and Micromechanics (BioSyM) IRG, Singapore-MIT Alliance for Research and Technology (SMART) Centre, Singapore

<sup>2</sup>School of Mechanical and Manufacturing Engineering, Australian Centre for NanoMedicine, University of New South Wales, Sydney, NSW 2052, Australia

<sup>3</sup>Mechanobiology Institute, National University of Singapore, Singapore

<sup>4</sup>Department of Biomedical Engineering, National University of Singapore, Singapore

<sup>5</sup>Department of Electrical Engineering and Computer Science, Department of Biological Engineering, Massachusetts Institute of Technology, Cambridge, Massachusetts, USA

# These authors contributed equally to this paper

\*Contact:

Jongyoon Han ([jyhan@mit.edu](mailto: jyhan@mit.edu))  
Room 36-841, Research Laboratory of Electronics,  
Massachusetts Institute of Technology  
77 Massachusetts Avenue, Cambridge, MA 02139, USA

Chwee Teck Lim ([ctim@nus.edu.sg](mailto: ctim@nus.edu.sg))  
Department of Biomedical Engineering, National University of Singapore,  
9 Engineering Drive 1, Singapore 117575, Singapore

## Abstract

Diagnosis of malaria at the early stage of infection is challenging due to difficulty in detecting the low abundance of parasites from blood. Molecular methods such as polymerase chain reaction (PCR) can be especially useful for detecting low parasitemia levels due to their high sensitivity and the ability to recognize different malarial species and strains. Unfortunately, the accuracy of PCR-based malaria detection can be compromised by many factors, including limited specificity of primers, presence of PCR inhibitors in blood serum and DNA contamination from nucleated blood cells. Here, we use a label-free, shear-modulated inertial microfluidic system to enrich malaria parasites from blood so as to facilitate a more reliable and specific PCR-based malaria detection. This technique capitalizes on cell focusing behaviors in high aspect ratio microchannels coupled with pinched flow dynamics to isolate malaria parasites from lysed blood containing white blood cells (WBCs). In this high aspect ratio (ratio of channel height to width) platform, the high shear rate along the channel width causes dispersed WBCs at the inlet to migrate and align into two streams near the channel sidewalls while the malaria parasites remain unfocused. Sensitive detection of parasites at spiked densities ranging from  $10^3$  to  $10^4$  *Plasmodium falciparum* parasites per mL ( $\sim 2$  per  $\mu\text{L}$ ) have been demonstrated and quantified in whole blood using quantitative PCR. This is approximately 100-fold more sensitive than the gold standard conventional microscopy analysis of thick blood smears. The simplicity of this device makes it ideal for integration with an automatic system for ultra-fast and accurate detection despite low levels of parasitemia. It can also help clinicians to monitor parasite survival in real-time during drug treatment and, if necessary adjust the treatment regimen.

**KEYWORDS:** *Microfluidics; Cell separation; Disease detection and diagnosis; Malaria; Blood; Plasmodium falciparum*

# Introduction

A total of five *Plasmodium* (*P.*) protozoa have been discovered to date which can infect humans with malaria via the *Anopheles* mosquito,<sup>1</sup> with infection by *P. falciparum* being the most extensive and deadly.<sup>2</sup> The *P. falciparum* infected red blood cells (iRBCs) undergo several developmental stages (ring, trophozoite and schizont) in a 48-hour intra-erythrocytic cycle. Consequently, the iRBCs undergo morphological changes that disrupt microcirculation,<sup>3, 4</sup> manifesting into anaemia and organ<sup>5</sup> failure in severe cases. Although some progress has been made in mitigating malaria, 1-2 million people still fall victim to this preventable disease annually.

The microscopic method remains the ‘gold’ standard test for malaria and is one of the most affordable means for malaria diagnosis. However, the staining and analysis processes require highly trained healthcare workers, particularly for accurate identification of species at low level parasitemia or in mixed malaria infections. A major drawback of microscopic examination is its relatively low sensitivity allowing the average microscopists to detect only 50-100 parasites/ $\mu$ L.<sup>6</sup> Additionally, there is frequent misinterpretation of microorganisms like bacteria such as *P.* protozoa.<sup>7</sup> Laboratory alternatives such as polymerase chain reaction (PCR) can also be used to diagnose malaria and are especially useful for detecting low parasitemia levels or mixed infections.<sup>8</sup> Unfortunately, the accuracy of PCR can be compromised by many factors such as nonspecificity of primers, present of PCR inhibitors in blood, and most importantly DNA contamination from nucleated blood cells.<sup>9</sup>

Various microfluidic platforms are under development to address a range of medical problems, particularly related to human diseases. The scale of microfluidic systems provides an ideal interface for manipulating cells and microorganisms with a precise control of spatial and temporal factors inside integrated systems having low mass-production costs.<sup>10, 11</sup> For example, Hou et al.,<sup>12</sup> made use of cell deformability and margination concept for the

separation of *P. falciparum*-infected red blood cells (iRBCs) from whole blood based on their reduced deformability. The reduction in deformability is also a physical phenomenon observed in other diseases including sickle cell disease which is equally prevalent in areas endemic with malaria. Interestingly, RBCs infected with *P. vivax* have reportedly increased deformability,<sup>13</sup> greatly discounting the use of deformability as a definitive biomarker for malaria diagnosis. Other groups have also explored the possibility of malaria detection using iRBC deformability.<sup>14-16</sup> Gascoyne and colleagues reported the possibility of using dielectrophoresis (DEP) to isolate iRBCs and proposed the combination of their system with a miniaturized PCR to form an integrated miniaturized system.<sup>17</sup> Other emerging technologies for malaria detection include using magnetic<sup>18</sup> and optical<sup>19</sup> means.

In this work, we make use of a label-free, shear-modulated inertial microfluidic system we reported earlier<sup>20</sup> to enable the enrichment and purification of malaria parasites from blood, which leads to more reliable and specific PCR-based malaria detection. The design consists of a single inlet high aspect ratio rectangular microchannel patterned with a contraction-expansion array with the following dimensions 30/90  $\mu\text{m}$  (contraction/expansion). The outlet opens into a 300  $\mu\text{m}$  wide section and is divided into three bifurcating arms, with two peripheral outlets and a central outlet. White blood cells (WBCs) which have comparable dimensions to the microchannels experience substantial inertial lift forces and migrate across the flow streams to be removed at the peripheral outlets while the malaria parasites are found in all outlets, mainly at center as they are not focused. Sensitive detection of parasites at spiked densities ranging from  $10^3$  to  $10^4$  *P. falciparum* parasites per mL ( $\sim 2$  per  $\mu\text{L}$ ) have been demonstrated and quantified in whole blood using qPCR. This is approximately 100-fold more sensitive than conventional microscopy analysis of thick blood smears. The simplicity of this device makes it ideal for integration to an automatic system with

downstream detection modules to ultimately create sample-to-answer microfluidic point of care (POC) diagnostics devices.

## Materials and methods

### Device design and fabrication

The microfluidic device consisted of a high aspect ratio single inlet rectangular microchannel patterned with a contraction-expansion array. We designed three different dimensions for the widths of the contraction-expansion array to check the performance of each in terms of WBC depletion and parasite recovery. The widths were fixed at 30/90  $\mu\text{m}$  (contraction/expansion), 40/120  $\mu\text{m}$ , and 50/150  $\mu\text{m}$ . The microchannel consisted of 85 subunits of contraction-expansion regions spanning a total length of 20 mm. The outlet opened into a 300  $\mu\text{m}$  wide section and was divided into two different designs in the ratio of 1:1:1 or 1:2:1 (top:middle:bottom). The latter design was designed to enhance the enrichment ratio as more parasites could be captured in the centre outlet. Nonetheless, this might compromise the purity as the WBCs might not be exactly focused at the channel walls and could escape into the centre outlet. The mold with its specific channel dimensions was designed and fabricated using conventional microfabrication technique described elsewhere.<sup>21</sup> The microfluidic biochips were fabricated by casting degassed polydimethylsiloxane polymer (mixed in the ratio of 10:1, Sylgard 184, Dow Corning, USA) on the patterned wafer and subsequent baked for 2 hr at 70 °C. After curing, the PDMS was peeled from the patterned wafer and access holes (1.5 mm) for fluidic inlets and outlets were punched using Uni-Core<sup>TM</sup> Puncher (Sigma-Aldrich Co. LLC. SG), and the PDMS devices were irreversibly bonded to glass using an oxygen plasma machine (Covance, FemtoScience, South Korea) to complete the channels. The assembled device was finally placed in an oven at 70 °C for 2 hr to further enhance the bonding.

### Device characterization

The microchannels were mounted on an inverted phase contrast microscope (Olympus IX71) coupled with a high speed CCD camera (Phantom v9, VisionResearch Inc., USA). The microfluidic chip was primed with buffer (1x PBS, 2mM EDTA supplemented with 0.5% BSA) using a syringe pump (PHD 2000, Harvard Apparatus, USA) for 2 min at a flow rate of 500  $\mu\text{L}/\text{min}$ . During testing, the samples were filled into 10 mL syringes and pumped through the microfluidic device via flexible Tygon<sup>®</sup> tubing. The flow rate was set to 400  $\mu\text{L}/\text{min}$  for the experiments involving malaria parasites. High speed videos were captured using the Phantom Camera Control software and analyzed subsequently with ImageJ software.

As a proof of concept, fluorescent beads of 1.5 and 9  $\mu\text{m}$  (Bangs Laboratories, USA) were used as a surrogate to simulate malaria parasites and WBCs, respectively. 1.5  $\mu\text{m}$  beads were used to simulate the malaria parasites as particles smaller than 1.5  $\mu\text{m}$  could not be visualized using the camera. Healthy blood samples were lysed with RBC lysis buffer (eBioscience, USA) according to the manufacturer's instruction to perform characterization tests. All lysed blood samples were diluted to 0.25x with 1x PBS before running through microfluidic device unless stated otherwise. After harvesting iRBCs from culture (see Supplementary info) thin Giemsa-blood smear test was performed to determine the parasitemia level using Olympus X71 microscope. Mapped image of 10  $\mu\text{L}$  iRBC suspension in haemocytometer was obtained to calculate the total cell count. The parasite count was determined by multiplying the total cell count with the parasitemia level. To mimic low levels of parasitemia, 2k-10k ring stage iRBCs (i.e., 1-10 parasites/ $\mu\text{L}$ ) were spiked into 1 mL of healthy blood and were lysed using 0.05% (w/v) Saponin (Sigma, USA). Saponin is able to disrupt the RBC membrane but leaves the malaria parasites membrane intact.<sup>22</sup> The suspension was then centrifuged at 2000 rpm for 5 min before washing with 1x PBS. Following lysis, diluted samples were run

through the microfluidic device. The samples were then collected from the outlets of the devices for PCR analysis.

### FACS analysis

The collection (1.5  $\mu\text{m}$  beads) and depletion (9  $\mu\text{m}$  beads) efficiencies of the devices were determined using BD<sup>TM</sup> Accuri C6 flow cytometer (BD Biosciences, USA). The beads were gated based on side scatter and fluorescence intensity. WBC contamination was determined through counting of allophycocyanin (APC)-conjugated CD45 marker (1:100, Miltenyi Biotec Asia Pacific, Singapore) stained WBCs from the centre outlet. Briefly, collected samples from the centre outlet were washed with 1x phosphate buffered saline (PBS) and centrifuged before incubating with APC-conjugated CD45 antibodies for 35 min in dark and ice. The samples were then centrifuged at 1200 rpm for 5 min and suspended into a 100  $\mu\text{L}$  suspension before being pipetted into a 96 well-plate. WBCs were counted with the aid of an inverted epi-fluorescent microscope (Olympus IX81) with motorized stage.

### Malaria culture

The *P. falciparum* 3D7 strain was used for this study. Parasites were cultured in vitro according to a conventional protocol<sup>1</sup>. Parasites were grown in human erythrocytes in RPMI 1640 medium (Sigma) supplemented with 0.5% Albumax I (Invitrogen), 2mM L-glutamin, 50  $\mu\text{g}/\text{ml}$  hypoxanthine and 25  $\mu\text{g}/\text{ml}$  gentamycin at 2.5% hematocrit and cultured at 5%  $\text{CO}_2$ , 3%  $\text{O}_2$  and 92%  $\text{N}_2$  at 37 °C. Synchronization of the culture was conducted every two days using 5% sobitol treatment<sup>2</sup> when the parasites were at the ring stage. Following the characterization of device, desired numbers of iRBCs were spiked into whole blood, mixed gently and lysed using saponin to extract the malaria parasite from iRBCs for subsequent detection (Fig. S1).



## PCR analysis

Enriched parasites concentrated into 200  $\mu\text{L}$  of PBS were processed with the Malaria Kit (Norgen, # 34800, Canada) according to the manufacturer's instructions for PCR evaluation. Real-time PCR was performed using a Step One Plus<sup>TM</sup> Detection System (Applied Biosystems, Foster City, CA) using SYBR Green (Invitrogen). PCR reactions were performed in a 96-well optical plate, with cyclical steps as follows: 95 °C for 3 min, followed by 40 cycles of 94 °C for 15 s and 60 °C for 30 s. The threshold cycle (CT) is defined as the fractional cycle number at which the fluorescence passed the fixed threshold. CT values data were obtained using default threshold settings. The melt curve analysis was obtained between 65 °C to 95 °C with a reading taken every 0.1 °C after holding the temperature for 5 s.

## Results and discussion

### Design Principle

Particles or cells flowing in a straight microchannel are subjected to hydrodynamic forces namely, the viscous drag and the inertial lift forces. The drag forces (i.e. due to the viscosity of the carrier fluid) are responsible for entraining particles along the flow streamlines while the inertial lift forces are responsible for the lateral migration of particles across the flow streamlines.<sup>23</sup> The balance of these forces drives particles to the side walls resulting in the equilibration of the uniformly dispersed cells/particles into a narrow band around the microchannel periphery.<sup>24, 25</sup> In the high aspect ratio (ratio of channel height to width) microfluidic channels, the high shear rate along the channel width causes dispersed WBCs at the inlet to migrate and align into two streams near the channel sidewalls (see Fig. 1B).<sup>20</sup> In this work, we take advantage of this phenomenon to focus all WBCs along the channel walls for downstream removal while the malaria parasites remain unfocused exiting from all outlets.

To maximize enrichment of parasites while reducing WBC contamination, a cascaded system was designed to perform 2-cycles enrichments (Fig. 1C).

### Characterization of chip performance with surrogate particles

In order to understand the effects of dimensions on the focusing behaviors of 9  $\mu\text{m}$  beads, a range of flow rates were tested. The optimized flow rates served as a starting point to predict the focusing behaviors of WBCs in future tests using blood. The 9  $\mu\text{m}$  beads were focused along the channel sidewalls at a flow rate of 300-1000  $\mu\text{L}/\text{min}$  for the 30/90  $\mu\text{m}$  design, 200-700  $\mu\text{L}/\text{min}$  for the 40/120  $\mu\text{m}$  design and 200-600  $\mu\text{L}/\text{min}$  for the 50/150  $\mu\text{m}$  design. When particle size becomes small as compared to microchannel dimensions, the balance between shear-modulated inertial lift and wall-induced lift forces is disrupted, causing disequilibrium of particles. As the widths of the contraction-expansion array increase, the tolerable flow rate for the 9  $\mu\text{m}$  beads to be focused therefore decreased.

FACS was used to determine collection efficiency of the 1.5  $\mu\text{m}$  beads and depletion efficiency of the 9  $\mu\text{m}$  beads (Fig. S2). Samples were run one cycle through a single device and two cycles through the cascaded system at 600  $\mu\text{L}/\text{min}$  (the maximum speed at which the 9  $\mu\text{m}$  beads were focused for all three device designs). In the single cycle run, the outlet ratio was 1:2:1. In the two cycles run, the outlet ratio of the pressure compensator was 1:2:1 while the other two chips had outlet ratio of 1:1:1. This particular arrangement was set up to boost the collection efficiency as a larger percentage of unfocused particles would be collected in the centre outlets in the 1:2:1 outlet design. In the cascaded system, the collection was from the centre outlet of stage 1 and stage 2 chips. The collection efficiency of the 1.5  $\mu\text{m}$  beads was around 50% for the single cycle run and 60% for the cascaded system (Fig. 2A). The cascaded system also improved the depletion efficiency (Fig. 2B). From the results, we determined that the device design of 50/150  $\mu\text{m}$  had the highest contamination for the 9  $\mu\text{m}$  beads, and hence this design was no longer characterized for WBCs isolation efficiency.

### Characterization of biochip performance with blood samples

From the previous tests, we eliminated the microfluidic device design of 50/150  $\mu\text{m}$  which had the highest contamination rate and continued to characterize devices with design of 30/90  $\mu\text{m}$  and 40/120  $\mu\text{m}$ . WBCs, unlike polystyrene beads, are much more deformable and exhibit greater variability in cellular sizes. Consequently, the range of flow rate for WBC equilibration decreases (Table S1). High speed videos showed that the device design of 30/90  $\mu\text{m}$  was better in minimizing WBCs contamination than the 40/120  $\mu\text{m}$  design (Fig. 2E), possibly as the dimensions of the former design were closer to the WBCs sizes. The outlet design of 1:1:1 was also found to deplete a larger number of WBCs than the 1:2:1 design. Thus, subsequent experiments were hence performed with only the 30/90  $\mu\text{m}$  design (Movie S1 and S2).

Tests were conducted to determine the highest blood concentration that can be processed in the microchannels without significantly compromising WBC depletion. Ideally, the application should work with undiluted blood to reduce processing and analysis time. Nonetheless, lysed blood still contains  $\sim 7 \times 10^6$  WBCs/mL that can contribute to cellular interactions and decrease the purity of the system. As shown in Fig. 2C, as the blood concentration decreased, the WBC depletion improved. The 0.25x diluted blood was found to satisfactorily remove 99.99% of WBCs. To minimize processing time while increasing the throughput, it is essential to process the blood samples at the highest flow rates. Experiments were performed to evaluate the WBC depletion rate as a function of Reynolds (Re) number.  $\text{Re} = 10.8$  corresponding to a flow rate of 400  $\mu\text{L}/\text{min}$  was found to remove 99.9% of the WBCs in a single run (Fig. 2D). The results suggested that an optimal range of flow rate between 300 – 450  $\mu\text{L}/\text{min}$  exists for WBC removal in the designed microchannels. The WBC depletion was around 99.90% and 99.99% for one and two cycles run through the 30/90  $\mu\text{m}$  design, respectively. This difference of  $\sim 0.09\%$  translates to a reduction of  $\sim 2000$

WBCs that can substantially improve the purity of the collected sample for subsequent downstream analysis such as PCR.<sup>26</sup> To compare the depletion efficiency of our system with available commercial kit for this purpose (i.e., CD45 coated beads, Miltenyi Biotec, USA) we have conducted a series of experiments using healthy blood samples. The obtained results (Fig. 3A) confirmed superior performance of the microfluidic chip both in terms of depletion efficiency and processing time. While there are reports that immunomagnetic separation can achieve depletion efficiency close to 99%,<sup>27</sup> these separations made use of conjugated antibodies that can increase the cost and affect the product shelf-life. Additionally, the presence of magnetic particles in the enriched samples can also significantly affect the PCR results.

### PCR analysis

Following the characterization of device dimensions and operating conditions, clinically relevant numbers of iRBCs ( $10^3$ - $10^4$  per mL) were spiked into whole blood to emulate the condition of low level parasitemia. Percentage recovery of iRBCs in both blood and PBS after microfluidics processing was estimated by the Ct values obtained from enriched samples in contrast to spiked iRBCs standards via real time PCR analysis. A range of standards were utilized, namely 2k-10k iRBCs, to plot the standard curve (Fig. 3B). This was carried out by establishing a linear fit with the values of known spiked count (x axis) and Ct values (y-axis). The specificity of the primers was confirmed by melt curve analysis (Fig. S3), as observed by the two peaks corresponding to spiked iRBCs and isoC control provided in the Malaria kit. Spiked iRBCs in 1 mL PBS (2-10k iRBCs) obtained an average recovery percentage of  $82 \pm 15.2\%$  while spiked iRBCs in 1 mL of blood yielded a mean of  $70.9 \pm 11.4\%$  (Fig. 3B). This is comparable to the value estimated via FACS with beads which was approximately 60%. To check the effect of nucleated cell removal on the PCR results, we also performed an off-chip

qPCR for a few samples without enrichment. Obtained results revealed that the sample preparation using the inertial microfluidic device can significantly enhance the PCR results (Fig. S4) and make it more reliable (see the threshold cycle (Ct) value of Fig. 3C) by removing most of the contaminants, such as leukocyte genomic materials and PCR inhibitors.

## Conclusions

Diagnosis of malaria at early stage remains challenging due to the intricacy of detecting low-density infections. The ability to isolate and enrich minute quantity of malaria parasites with a high degree of purity from *P. falciparum* infected blood provides a tool to enhance diagnostic and detection efficiency of molecular assays. Here, a highly efficient inertial microfluidic device was developed to enrich and purify malaria parasites from blood, which leads to more reliable and specific PCR-based malaria detection. The device makes use of equilibrium between shear-modulated inertial lift and wall-induced lift forces to remove WBCs, thereby facilitating malaria parasite enrichment. The suitability of six different designs was assessed using fluorescent beads and malaria parasites spiked in both PBS solution and lysed blood. The microfluidic device of dimensions 30/90  $\mu\text{m}$  with outlet ratio of 1:1:1 had the most ideal performance of 99.99% WBCs depletion and malaria parasites collection yield of  $70.9 \pm 11.4\%$  after two cycles run. Although blood dilution is needed, the elegant design of the microchannel allows for easy parallelization to form a cascaded system. The cascaded system is able to process 1 mL of lysed blood in 15 min making it an ideal platform for WBCs depletion comparing to the existing techniques. The WBC depletion efficiency was around 99.99% which is much higher than any commercially available kit (i.e., CD-45 coated beads) for this purpose. Parasite densities ranging from  $10^3$  to  $10^4$  *P. falciparum* parasites per mL ( $\sim 2$  per  $\mu\text{L}$ ) have been demonstrated and quantified in whole blood using qPCR. Obtained results revealed that the sample preparation using the inertial

microfluidic device can significantly enhance the PCR results and make it more reliable by removing most of the interfering genomic materials and PCR inhibitors. Although some malaria parasites are lost during the processing, the enriched sample is more useful for subsequent analytical work. We expect that a  $\mu$ TAS for malaria parasite study and diagnosis can be created by integrating chip-based analysis downstream of the microfluidic device. Beyond the isolation of malaria parasites, this microfluidic platform may also be extended to other applications such as bacteria isolation and enrichment.

### Acknowledgements

Financial support by the Singapore-MIT Alliance for Research and Technology (SMART) Centre (BioSyM IRG) is gratefully acknowledged. Assistance in terms of advice and equipment use from Patrick Doyle group (SMART) for PCR and gel analysis is greatly appreciated. We would also like to thank Dr. Ali Asgar S. Bhagat for his advice during the initial phase of the device design. This work is supported by the use of facilities for wafer fabrication at the Mechanobiology Institute, National University of Singapore as well as at the Nanyang Technological University. The use of lab facilities at the Infectious Disease Program (ID IRG) at SMART and the Nano Biomechanics Laboratory at the National University of Singapore is also gratefully acknowledged.

### References

1. N. White, *Clinical infectious diseases*, 2008, 46, 172-173.
2. Y. Lim, R. Mahmud, C. Chew, T. Thiruvethiran and K. Chua, *Malaria journal*, 2010, 9, 272.
3. A. G. Maier, B. M. Cooke, A. F. Cowman and L. Tilley, *Nature Reviews Microbiology*, 2009, 7, 341-354.
4. S. J. ROGERSON, G. E. GRAU and N. H. HUNT, *Microcirculation*, 2004, 11, 559-576.
5. A. Dondorp, B. Angus, K. Chotivanich, K. Silamut, R. Ruangveerayuth, M. Hardeman, P. Kager, J. Vreeken and N. White, *On the pathophysiology of severe falciparum malaria with special reference*, 1997, 57, 69.
6. N. Tangpukdee, C. Duangdee, P. Wilairatana and S. Krudsood, *The Korean journal of parasitology*, 2009, 47, 93-102.

7. L. K. Erdman and K. C. Kain, *Travel medicine and infectious disease*, 2008, 6, 82-99.
8. M. Makler, C. Palmer and A. Ager, *Annals of tropical medicine and parasitology*, 1998, 92, 419-433.
9. T. Hänscheid and M. P. Grobusch, *Trends in parasitology*, 2002, 18, 395-398.
10. E. W. Majid and C. T. Lim, *Microfluidic Platforms for Human Disease Cell Mechanics Studies*, Springer, 2013.
11. A. A. Bhagat, H. Bow, H. W. Hou, S. J. Tan, J. Han and C. T. Lim, *Medical & biological engineering & computing*, 2010, 48, 999-1014.
12. H. W. Hou, A. A. S. Bhagat, A. G. L. Chong, P. Mao, K. S. W. Tan, J. Han and C. T. Lim, *Lab on a Chip*, 2010, 10, 2605-2613.
13. S. Handayani, D. T. Chiu, E. Tjitra, J. S. Kuo, D. Lampah, E. Kenangalem, L. Renia, G. Snounou, R. N. Price and N. M. Anstey, *Journal of Infectious Diseases*, 2009, 199, 445-450.
14. H. Bow, I. V. Pivkin, M. Diez-Silva, S. J. Goldfless, M. Dao, J. C. Niles, S. Suresh and J. Han, *Lab on a Chip*, 2011, 11, 1065-1073.
15. Q. Guo, S. J. Reiling, P. Rohrbach and H. Ma, *Lab on a Chip*, 2012, 12, 1143-1150.
16. J. P. Shelby, J. White, K. Ganesan, P. K. Rathod and D. T. Chiu, *Proceedings of the National Academy of Sciences*, 2003, 100, 14618-14622.
17. P. Gascoyne, J. Satayavivad and M. Ruchirawat, *Acta tropica*, 2004, 89, 357-369.
18. J. Nam, H. Huang, H. Lim, C. Lim and S. Shin, *Analytical Chemistry*, 2013, 85, 7316-7323.
19. S. A. Lee, R. Leitaog, G. Zheng, S. Yang, A. Rodriguez and C. Yang, *PloS one*, 2011, 6, e26127.
20. A. A. S. Bhagat, H. W. Hou, L. D. Li, C. T. Lim and J. Han, *Lab on a Chip*, 2011, 11, 1870-1878.
21. M. E. Warkiani, B. L. Khoo, D. S.-W. Tan, A. A. S. Bhagat, W.-T. Lim, Y. S. Yap, S. C. Lee, R. A. Soo, J. Han and C. T. Lim, *Analyst*, 2014, 139, 3245-3255.
22. R. J. Allen and K. Kirk, *Journal of Biological Chemistry*, 2004, 279, 11264-11272.
23. B. Khoo, M. Warkiani, G. Guan, D. S.-W. Tan, A. S. Lim, W.-T. Lim, Y. S. Yap, S. C. Lee, R. A. Soo and J. Han, 2014.
24. A. A. S. Bhagat, S. S. Kuntaegowdanahalli and I. Papautsky, *Microfluidics and nanofluidics*, 2009, 7, 217-226.
25. J. Zhou, P. V. Giridhar, S. Kasper and I. Papautsky, *Lab on a Chip*, 2013, 13, 1919-1929.
26. A. M. Sieuwerts, J. Kraan, J. Bolt-de Vries, P. van der Spoel, B. Mostert, J. W. Martens, J.-W. Gratama, S. Sleijfer and J. A. Foekens, *Breast cancer research and treatment*, 2009, 118, 455-468.
27. O. Lara, X. Tong, M. Zborowski and J. J. Chalmers, *Experimental hematology*, 2004, 32, 891-904.



## Figure captions

**Figure 1.** (A) Sample processing workflow showing different steps. The blood sample is collected; RBCs along with iRBCs are lysed and processed through cascaded microfluidics chip. The isolated parasites with high purity are available for quantitative measurement and detection using PCR. (B) Schematic representation of the configuration and operational mechanism of the designed microfluidic chip for enrichment of malaria parasite. The device consists of a contraction-expansion array spanning a total length of 20 mm before expanding into three outlets. Particles larger than 4  $\mu\text{m}$  such as WBCs are focused along the channel walls and are isolated via the peripheral outlets. The malaria parasites, on the other hand, are unfocused and are distributed in all the three outlets. (C) Optical pictures showing the actual cascaded device for enrichment of parasites in two stages. The set-up consists of three biochips connected together, with one chip functioning as a pressure compensator.

**Figure 2.** (A) Particle counting results showing the collection efficiency of the 1.5  $\mu\text{m}$  beads for various designs. Flow cytometry data revealed that the efficiency of separation for the 30/90  $\mu\text{m}$  1:1:1 biochip was around 50% for the single cycle run while that for the two cycles run was close to 60%. (B) Particle counting results representing the depletion efficiency of the 9  $\mu\text{m}$  beads for all three different designs (> 96% for all designs). However, based on the least desirable results from the 50/150  $\mu\text{m}$  design, only the remaining designs were further characterized with WBCs. (C) Investigation of WBC depletion as a function of sample concentration. The depletion efficiency increased as the dilution factor increased. The 0.25x diluted blood (i.e., 4 times dilution) yielded a 99.90% reduction in WBC count. (D) WBC depletion efficiency as a function of  $Re$  number. The most efficient depletion efficiency was at  $Re = 102.5$  corresponding to a flow rate of around 400  $\mu\text{L}/\text{min}$ . (E) Further characterization of the devices using high speed microscopic images. The 30/90  $\mu\text{m}$  (1:1:1) design showed the best performance in reducing WBC contamination from the sample. The yellow arrows indicate WBCs escaping into the centre outlets due to compromised focusing behaviors. The 1:2:1 outlet allowed more WBCs to escape into the centre outlet.

**Figure 3.** (A) A comparison of WBC depletion efficiency of our device and CD-45 coated magnetic beads. The processing time for the microfluidic device is around 15 min (1mL blood) while it takes about 90 min for the commercial kit to deplete leukocytes. (B) Quantitative PCR analysis to check the efficiency of separation of our device. Recovery percentage of malaria parasites spiked in PBS and blood was  $82 \pm 15.2\%$  while spiked iRBCs in 1 mL of blood yielded a mean of  $70.9 \pm 11.4\%$ , respectively. (C) Ct value data demonstrating the efficacy of our device for the PCR sample preparation. These data clearly show that detection of low levels of parasitemia (2k per mL) using the commercial kit directly from blood is technically impossible; however, this can be done easily by removing the entire WBCs from the sample using our microfluidic system.



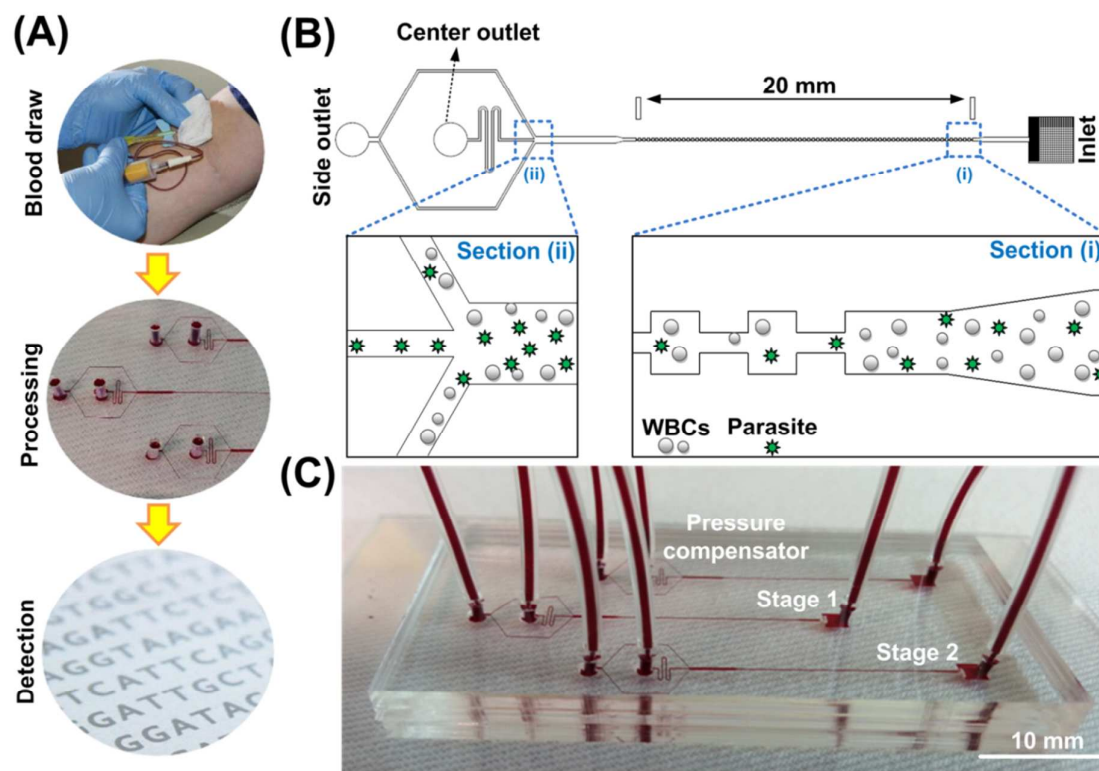
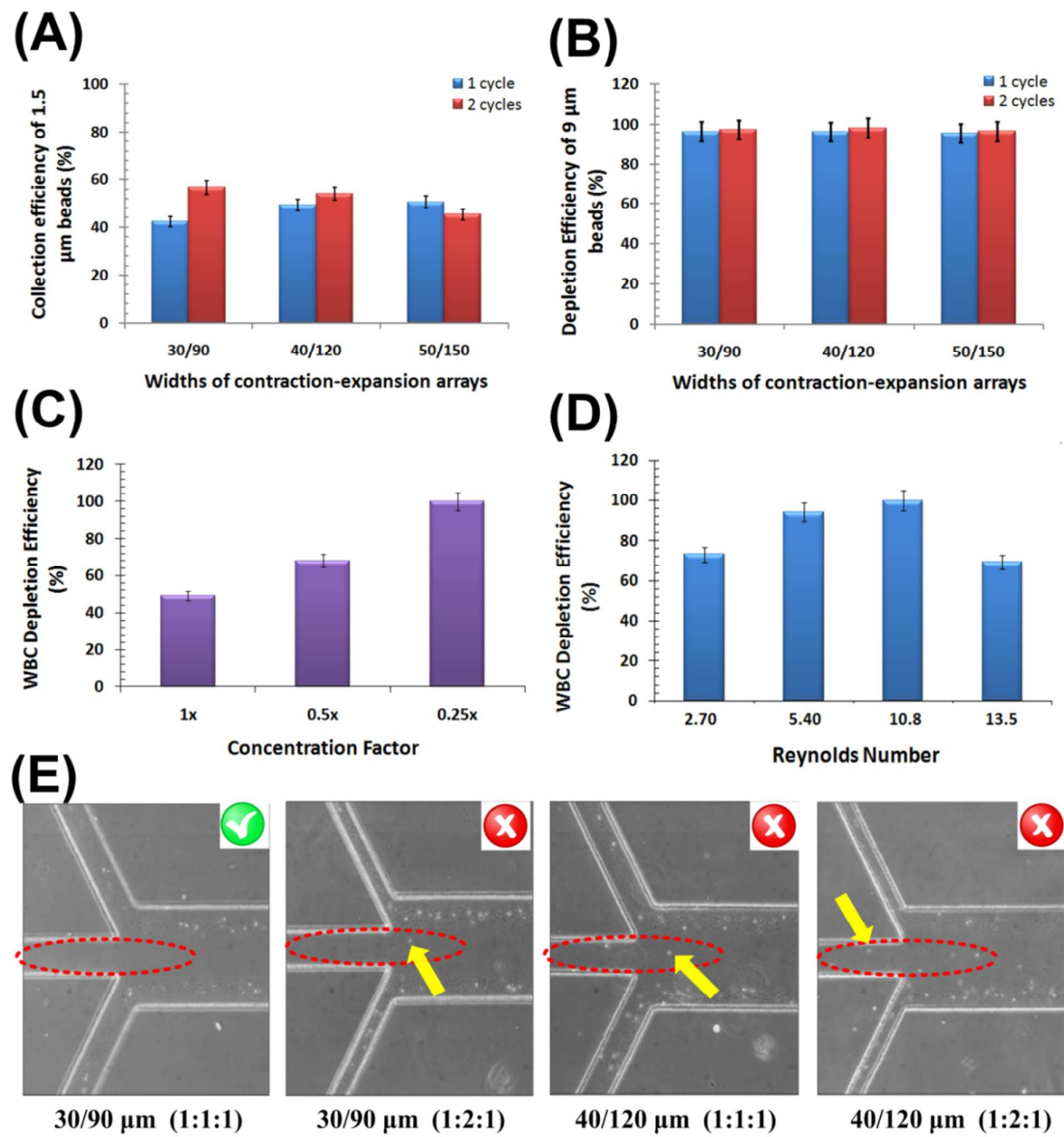
**Figure 1**

Figure 2



**Figure 3**